



ELSEVIER

Solar Energy Materials and Solar Cells 36 (1995) 169–185

Solar Energy Materials
and Solar Cells

Microwave detection of minority carriers in solar cell silicon wafers

J.A. Eikelboom ^{*}, C. Leguijt, C.F.A. Frumau, A.R. Burgers

Netherlands Energy Research Foundation ECN, P.O. Box 1, 1755 ZG Petten, The Netherlands

Received 12 August 1993; revised 3 June 1994

Abstract

Techniques measuring photoconductive decay by means of microwaves (μ -PCD) can be used to detect free carriers in semiconductors. The instrument as developed at ECN for characterization of the solar cell material is described. The experimental details of two measurement techniques and the theoretical background are discussed. In the decay method the effective mean lifetime of the minority carriers is measured. In the harmonic modulation technique information about the lifetime of the minorities is contained in the phase-shift of the microwave signal relative to the phase of the light intensity. The aim of this research is to determine the bulk mean lifetime of the minority carriers and the surface recombination velocities of solar cell silicon wafers by a non-destructive and contactless technique. Typical experiments will be presented.

1. Introduction

The efficiency of a silicon solar cell depends on a number of physical parameters, which characterize the semiconductor material from which it is made. In the global effort to improve the efficiency of mass-produced and low-priced solar cells there is a clear need for an experimental technique which would allow contactless and non-destructive measurement of these parameters. The crucial parameters of the semiconductor are the bulk mean lifetime τ_b of the minority carriers and the recombination rates S_1 and S_2 on the front and the back surface of the wafer.

The requirement that the desired technique is contactless rules out a number of commonly used techniques, such as current decay methods where wire contacts

^{*} Corresponding author.

have to be made. Many of these techniques demand the presence of a junction in the semiconductor.

The technique based on the reflection of microwaves by the free carriers in the material is contactless and requires no junction. It allows straightforward measurement of the mean lifetime of minority carriers in silicon wafers. Wafers can be taken out of the production process of solar cells for quality control and can be measured within minutes. As the experiment does not influence the basic properties of the wafer, it can be processed further to be measured again at a later stage.

The use of microwaves to detect free carriers in semiconductors has been known for several decades. Different arrangements have been used according to the component availability and the desired frequency, see Refs. [1]–[5]. The frequency range is from 1 GHz up to 40 GHz, using transmission lines up to 4 GHz and wave guides at the higher frequencies. The instrument used at our institute is based on a design developed at the Physics Laboratories of Philips Industries in The Netherlands in cooperation with the University of Delft. The University of Delft developed the design into an instrument which could be used in their research program, in which high quality silicon wafers for sensors were tested, see Refs. [2],[3].

The instrument at the ECN laboratory for the characterization of solar cells is based on the Delft design. The silicon wafers commonly used for solar cells are not made of high quality monocrystalline material. The low quality PV-grade semicrystalline wafers pose new exigencies on the instrument.

2. General principles

An electromagnetic wave travelling in a conducting medium will be attenuated in accordance with the Maxwell equations. The attenuation distance or skin depth is a function of the conductivity σ , ϵ_r , and μ_r of the medium. In general, metals reflect electromagnetic waves very well. Electromagnetic waves can penetrate much deeper in materials with low values of σ , such as glass.

Besides metals and insulators such as glass, there are semiconductor materials which have intermediate values of σ . The conductivity of a material is determined by the concentration of free carriers, such as electrons in metals. In a pure semiconductor the concentration of free carriers is low, but the addition of small amounts of impurities can increase these concentrations enormously. Illumination of the semiconductor is another method to increase the concentration of free carriers. The photons are absorbed in the material and create free electrons and free holes. Microwaves are reflected by these free carriers.

The reflection coefficient R is defined as the fraction of the incident microwave power which is reflected by the wafer. Fig. 1 shows the reflection coefficient of a silicon wafer of thickness 100, 200 and 400 μm as a function of the resistivity $\rho = 1/\sigma$ of the material. The microwaves have a constant frequency of 2.8 GHz. Thick samples reflect more power than thin wafers and the reflection increases with decreasing resistivity. It is found that the reflection coefficient changes most

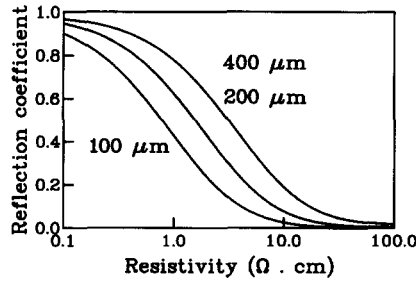


Fig. 1. Reflection coefficient as a function of the resistivity and the thickness of a silicon wafer.

rapidly in the range of $0.5 \Omega \text{ cm}$ to $5 \Omega \text{ cm}$, which coincides with the range of resistivity of the basic solar cell material. The reflection coefficient was calculated by solving the Maxwell equations assuming that the conductivity of the material is homogeneous over the volume of the wafer where microwaves are reflected.

When a silicon wafer is illuminated from one side the free carrier concentration will not be homogeneous, but it will be a function of the penetration z , i.e. $\sigma(z)$. The penetration depth of visible light in silicon is typically of the order of tens of micrometers. Otaredian [3] has shown that the reflection coefficient $R(\langle\sigma\rangle)$ calculated for the mean value of the conductivity is a good approximation for the numerically solved value $R(\sigma(z))$ for a non-homogeneous distribution of the conductivity.

In microwave reflection experiments the intensity of the illumination is not constant but modulated. This light modulation will induce a modulation $\Delta\sigma(x,t)$. Now the assumption is that in our experiment the illumination is such that the induced increase $\langle\Delta\sigma\rangle$ is small in comparison to $\langle\sigma\rangle$, so that we can write

$$R(\langle\sigma_0\rangle + \langle\Delta\sigma\rangle) - R(\langle\sigma_0\rangle) = \left. \frac{\partial R}{\partial \sigma} \right|_{\sigma=\langle\sigma_0\rangle} \langle\Delta\sigma\rangle \quad (1)$$

This means that the increase in the reflected power is proportional to the increase in the mean conductivity. The constant $\partial R/\partial \sigma$ is related to the inclination of the curves in Fig. 1. It is clear that the approximation breaks down for large $\Delta\sigma$, as the inclination is no longer constant. A fundamental reason for keeping $\Delta\sigma$ small is the fact that in the derivation of formulas for R are based on solving the Maxwell equations taking the conductivity σ time independent.

For frequencies other than 2.8 GHz curves like Fig. 1 can be drawn. It can be shown that the frequency of 2.8 GHz is a good choice for our conductivity range of interest [3]. The sensitivity of the instrument is proportional to the constant $\partial R/\partial \sigma$, which is near the maximum in this range.

In the experiments the microwaves are emitted by an antenna and partly reflected by a semiconductor wafer. The wafer is illuminated by a light source emitting monochromatic light, usually in the infrared range. The modulated light is absorbed by the wafer and the free carriers, which are generated, reflect the

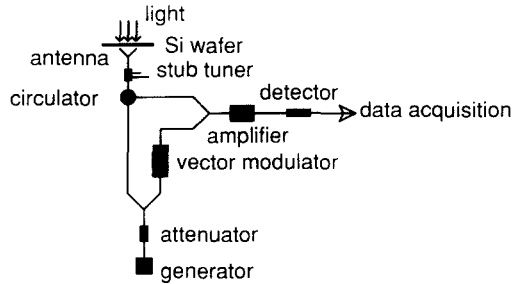


Fig. 2. Schematic layout of microwave reflection instrument.

incident microwaves, which are again absorbed by the antenna. The microwave power that is returned by the antenna into the transmission line consists of a DC and an AC part. The constant DC signal in part originates from the free carriers in the wafer which are present irrespective of the modulated illumination. Reflection by the antenna because of load mismatch and reflection on the front and back surface of the wafer also contribute to the constant DC signal.

The DC fraction contains no information about the bulk processes in the wafer. The AC modulation of the microwave signal is caused by the modulation of the light intensity. In our equipment it is at most a few percent of the DC part. In order to eliminate the DC part as far as possible a balanced bridge set-up is used [6]. Fig. 2 shows the schematic layout of the instrument.

A generator sends a microwave signal into a transmission line at a fixed frequency of 2.8 GHz. The signal is split in two parts. One half continues towards the antenna, the second half passes a device that can attenuate the signal and can change its phase. The signal which is returned from the antenna is directed by the circulator into a transmission line where it is combined with the attenuated and phase-shifted generator signal. This small signal which results from this addition is amplified and the result is the input signal for the detector. For the case where there is no light modulation on the wafer the attenuation and phase-shift are set in such a position that the detector senses a minimal signal. This means both signals are of the same amplitude but have opposite phase. When the wafer is illuminated by the modulated light a modulated signal is seen at the detector, which is proportional to the AC part of the microwave signal. Data acquisition can be performed by oscilloscope or lock-in amplifier.

3. Theory of photoconductivity modulation

3.1. The microwave signal

Consider a silicon wafer of thickness d which is illuminated by monochromatic light. During the measurement the excess carrier distribution can be described by a

function $n(x, t)$. In general the function is non-homogeneous in space and changing in time.

Normally it is tacitly assumed that the detected microwave signal is proportional to the mean free carrier concentration. Detailed analysis of the microwave signal reflected from different depths in the wafer with a fast changing distribution showed that interference effects change this simple picture [7]. When the thickness of the wafer becomes of the order of magnitude of the microwave wavelength and the wafer is illuminated by a short laserpulse, the intensity of the decaying microwave signal may not be proportional to the mean free carrier concentration. In our situation the relatively low frequency of the microwave signal, the thin wafers and the light pulses of long duration are such that these effects will play no significant role in our system. Therefore, we assume that the microwave signal as measured by our instruments is a linear function of the excess carrier distribution $n(x, t)$. We define the operator M as

$$M(n(x, t)) = \frac{1}{d} \int_0^d n(x', t) dx'. \quad (2)$$

The microwave signal is proportional to $M(n(x, t))$.

3.2. Absorption of light

The silicon wafer has an absorption coefficient a for the specific wavelength of the light used. The photonflux is N ($\text{cm}^{-2} \text{s}^{-1}$). When the photons have an energy greater than the bandgap of silicon, part of them is absorbed as they penetrate the material. An absorbed photon can create a free electron and a free hole, one of them being a minority carrier. The internal quantum efficiency ζ is the average number of minority carriers generated per absorbed photon. The intensity of the light decreases with the penetration depth. The excess free carriers are therefore generated non-homogeneously throughout the wafer. The generation rate $G(x, t)$ can be written as $g(x)h(t)$, $g(x)$ is given by

$$g(x) = k_1 e^{-ax} + k_2 e^{a(x-d)}. \quad (3)$$

The term $k_2 e^{a(x-d)}$ indicates that there is reflection of light at the back surface. The constants k_1 and k_2 depend on the photonflux N , the internal reflection coefficient R of the wafer, its thickness d and the absorption coefficient a of the material. They are given by

$$k_1 = \frac{a(1-R)}{1-R^2 e^{-2ad}} N \zeta, \quad (4)$$

$$k_2 = k_1 R e^{-2ad}. \quad (5)$$

3.3. The excess carrier distribution

As soon as they are created the free carriers start to move. There are two mechanisms: drift due to an electric field and diffusion due to a gradient in the

concentration. Normally there is only an electric field at a p-n junction, which means that in the bulk of the material diffusion currents are dominant.

At the same time the carriers can recombine at specific recombination centers in the bulk and on the surface of the semiconductor. The decay of the carriers can be modelled making a number of assumptions. The rate at which the minority carriers recombine in the bulk (in absence of diffusion) is assumed to be proportional to the excess concentration:

$$-\frac{\partial n(x,t)}{\partial t} = \frac{n(x,t)}{\tau_b}, \quad (6)$$

where τ_b is called the bulk mean lifetime of the carriers. In the experiments described here the aim is to remain always in low injection conditions, i.e., the amount of free charge created by incident light is negligible in comparison to the amount available through the doping of the wafer.

Normally there are many recombination sites on the surface of the semiconductor. The flow of carriers towards these sites is determined by the concentration gradient

$$J(x,t) = D \frac{\partial n(x,t)}{\partial x}, \quad (7)$$

where D is the diffusion coefficient of the minority carriers. In our model we assume that this flow of carriers is proportional to the concentration at the surface

$$D \frac{\partial n(x,t)}{\partial x} \Big|_{x=0} = S_1 n(0,t), \quad (8)$$

$$D \frac{\partial n(x,t)}{\partial x} \Big|_{x=d} = -S_2 n(d,t), \quad (9)$$

where S_1 and S_2 are the surface recombination rates at the front ($x=0$) and at the back surface of a wafer of thickness $x=d$. So the rate at which the minority carriers recombine is given by

$$\frac{\partial n(x,t)}{\partial t} = D \frac{\partial^2 n(x,t)}{\partial x^2} - \frac{n(x,t)}{\tau_b} = F(n(x,t)). \quad (10)$$

F defined here as a function operator. The concentration $n(x,t)$ is given by the differential equation

$$\frac{\partial n(x,t)}{\partial t} = F(n(x,t)) + g(x)h(t), \quad (11)$$

with the boundary conditions from Eqs. (8) and (9). First we solve this equation for the case where there is no generation of excess carriers, $g(x)h(t)=0$, i.e., the light has been turned off. Eq. (11) can be solved by separation of parameters

$$n(x,t) = T_i(t)e_i(x). \quad (12)$$

We find

$$\frac{T_i'(t)}{T_i(t)} = \frac{F(e_i(x))}{e_i(x)} = \lambda_i. \quad (13)$$

The functions $e_i(x)$ are orthogonal eigenfunctions of the operator F and the constants λ_i are the corresponding eigenvalues, where the innerproduct of two functions u and v on the interval $[0, d]$ is defined as

$$(u, v) = \frac{1}{d} \int_0^d u(x)v(x) dx. \quad (14)$$

When we define $\tau_i = -1/\lambda_i$ the function $T_i(t)$ is given by

$$T_i(t) = \exp\left(\frac{-t}{\tau_i}\right). \quad (15)$$

The eigenfunctions $e_i(x)$ have the general form

$$e_i(x) = \sin\left(\frac{\alpha_i x}{d} + \phi_i\right). \quad (16)$$

Thus, we find

$$\frac{1}{\tau_i} = \frac{1}{\tau_b} + \frac{D\alpha_i^2}{d^2}. \quad (17)$$

The constants α_i are determined by the surface recombination velocities S_1 and S_2

$$\tan(\alpha_i d) = \frac{D\alpha_i(S_1 + S_2)}{D^2\alpha_i^2 - S_1 S_2}. \quad (18)$$

3.4. The steady state distribution

Now we turn to the case where the wafer is illuminated by light with a certain constant intensity. The generation term $G(x, t)$ can be written as $g(x)$ and after some time the carrier distribution will reach a steady state $n(x)$. $n(x)$ is the solution of

$$D \frac{\partial^2 n(x)}{\partial x^2} - \frac{n(x)}{\tau_b} + g(x) = 0, \quad (19)$$

where $g(x)$ is the time-independent generation term, see Eq. (3). The general shape of the solution of this differential equation can be written in analytical form

$$n(x) = A \cosh(x/L) + B \sinh(x/L) + \frac{\tau_b}{1 - L^2 a^2} g(x), \quad (20)$$

where L is the diffusion length of the minority carriers, $L = \sqrt{\tau_b D}$. The constants A and B are determined by the boundary conditions at the surfaces, i.e., S_1 and S_2 . Fig. 3 shows the steady state solution for a silicon wafer of thickness 300 μm

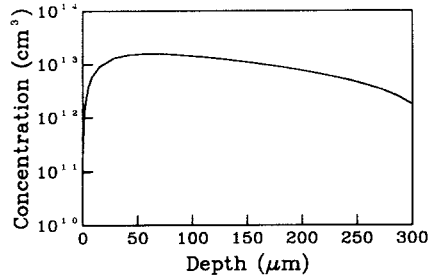


Fig. 3. Steady-state minority carrier distribution in a Si wafer of thickness 300 with $\tau_b = 20 \mu\text{s}$, $S_1 = 10^7 \text{ cm/s}$ and $S_2 = 10^4 \text{ cm/s}$.

with $\tau_b = 20 \mu\text{s}$, $S_1 = 10^7 \text{ cm/s}$ and $S_2 = 10^4 \text{ cm/s}$ illuminated with monochromatic light, $\lambda = 848 \text{ nm}$ and power 300 mW/cm^2 .

As the typical doping concentration is about 10^{16} per cm^3 it is clear that $n(x)$ is small compared to the total minority carrier concentration. This is the so-called low injection condition.

The solution $n(x)$ of Eq. (19) can also be written in terms of the eigenfunctions $e_i(x)$

$$n(x) = \sum_{i=1}^{\infty} \beta_i e_i(x). \quad (21)$$

The coefficients β_i can be determined using the fact that the functions $e_i(x)$ are orthogonal, see Eq. (14),

$$\beta_i = \tau_i \frac{(e_i(x), g(x))}{(e_i(x), e_i(x))}. \quad (22)$$

3.5. Pulsed light

Now we will study the decay of the excess carrier concentration after the light intensity was decreased instantaneously from $h(t) = 1$ for $t < 0$ to zero, i.e., $h(t) = 0$ for $t > 0$. We assume that the minority carrier distribution reached a steady state situation, like in Fig. 3, before this step. During this decay the carrier distribution $n(x, t)$ can be written as

$$n(x, t) = \sum_{i=1}^{\infty} \beta_i T_i(t) e_i(x) = \sum_{i=1}^{\infty} \tau_i \frac{(e_i, g)}{(e_i, e_i)} \exp\left(\frac{-t}{\tau_i}\right) e_i(x). \quad (23)$$

Eq. (23) shows that the decay will be a sum of exponential decays with increasing τ_i 's, although there is a unique bulk mean lifetime τ_b . After a time interval of the order of magnitude of the dominant decay has a mean lifetime of τ_1 . The coefficients β_i are equal to those in Eq. (21). If the light intensity is reduced not to zero but to a lower level $h(t) = h_2 \neq 0$ for $t > 0$, the carrier

concentration $n(x,t)$ will decrease to a new non-zero steady state distribution. $n(x,t)$ can be written as $n(x,t) = \Delta n(x,t) + n_0$, where $\Delta n(x,t)$ is given by Eq. (23) with different coefficients β_i .

Usually microwave reflection measurements consist of measuring the value of the largest of the decay times τ_i , which is τ_1 , the decay time of the fundamental mode. The value of τ_1 is determined by the fundamental parameters S_1 , S_2 and τ_b . The theory shows that the higher modes will be present in the initial part of the decay. These modes will extinguish faster than the fundamental mode, so in the tail of the decay one can fit an exponential function to the measured data and so determine τ_1 . When the decay starts from a steady state carrier distribution, i.e., after a light pulse of duration longer than τ_1 , hardly any initial decay is visible. In systems that operate with pulsed lasers, the contribution of the higher modes is much larger in the initial stage of the decay.

Although the presence of the higher modes contains information about the recombination rate at the front and back surface [4], it is in practice difficult to extract this information from the measurements. Accurate measurement of the initial decay is hampered by the finite transition time of the light pulse and the response time of the electronic equipment. Fundamental considerations concerning the phase of the reflected microwave signal, as were mentioned in the beginning of this section [7], add on to this, e.g., during the initial decay the microwave signal might not be proportional to the instantaneous mean free carrier concentration.

So in practice the measurement starts at the point in the decay where the carrier distribution function has lost all information about the wavelength of the light and the specific surface of the wafer which was turned towards the light source. The same value for τ_1 will be measured when the wafer is turned around and illuminated on the same spot, even when the recombination rates S_1 and S_2 on the opposite surfaces are vastly different.

In a later section it will be explained how the parameters S_1 , S_2 and τ_b can be determined from the measured τ_1 value in specific circumstances.

3.6. Harmonic modulation

When the light intensity does not change abruptly between fixed levels, but is modulated harmonically, the microwave signal will also show a sine variation. In general there will be a phase-shift between the microwave signal and the light signal which is determined by the fundamental wafer parameters [8]. The time dependence of the generation function $G(x,t)$ can be written as $h(t) = 1 + a \cos(\omega t)$.

The microwave signal contains a DC and an AC part. The DC part can be calculated from the steady state distribution corresponding to $h(t) = 1$. We will focus here on the AC part and will take $h(t) = \cos(\omega t) = \text{Re}(e^{i\omega t})$. As a general solution we take

$$n(x,t) = - \sum_i \gamma_i e^{i\omega t} e_i(x). \quad (24)$$

Note that $n(x, t)$ and γ_i are complex. For γ_i the following expression is found:

$$\gamma_i = \frac{\tau_i}{1 + i\omega\tau_i} \frac{(e_i, g)}{(e_i, e_i)}. \quad (25)$$

The microwave signal (Eq. (2)) is calculated to be

$$M(n(x, t)) = - \sum_i \gamma_i M(e_i) e^{i\omega t} \quad (26)$$

$$= B e^{i(\omega t + \phi)}, \quad (27)$$

with

$$\tan(\phi) = \arg\left(\sum_i \gamma_i M(e_i)\right), \quad (28)$$

$$B = \left| \sum_i \gamma_i M(e_i) \right|. \quad (29)$$

The phase of the microwave signal is shifted by $\phi(\omega)$ relative to the light modulation. It is possible to derive analytical expressions for $\phi(\omega)$ [8]. All the modes contribute to the microwave signal with a specific phase-shift and amplitude. The effective phase-shift is negligible for $\omega \ll 1/\tau_1$. As the modulation frequency is increased the phase-shift will increase also.

The fundamental difference with the decay method is that in this measured signal all higher modes remain present with a certain amplitude. This means that the amplitude B and the phase ϕ of the signal depend on the wavelength of the light signal and the recombination velocities on the front and back surface.

Now if the microwave signal decay after a light pulse would be a pure exponential process (i.e., $S_1 = S_2 = 0$, $g(x)$ constant), then a harmonically modulated microwave signal would be obtained for a harmonic light modulation and it would have a phase-shift ϕ related to the lifetime τ_b and the modulation frequency ω by

$$\tan(\phi) = \tau_b \omega. \quad (30)$$

This phase-shift, which is a function of the frequency, can be measured very accurately by a lock-in amplifier. We define the effective harmonic lifetime τ_h as $\tau_h = 1/\omega_h$, where ω_h is the frequency at which a phase-shift of 45° is observed between the microwave signal and the light intensity modulation.

Due to the non-homogeneous carrier generation and the non-zero surface recombination velocities the measured value of τ_h is different from τ_b as well as from τ_1 . This makes the choice of 45° in the definition of τ_h somewhat arbitrary. For every frequency ω there is a unique phase-shift ϕ , which is determined by the fundamental wafer parameters. The fact that τ_h is always smaller than τ_b and that it is of the order of magnitude of τ_1 makes it a useful parameter. For well passivated surfaces τ_h can serve as a good approximation of τ_b .

As mentioned above the value of τ_h contains more information than τ_1 . In contrast to τ_1 the value of τ_h depends on the wavelength of the incident light. For

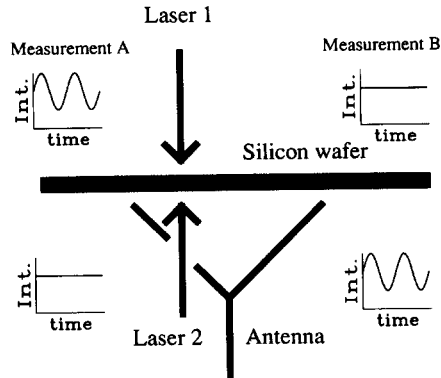


Fig. 4. Measurement procedure for bifacial measurements.

a wafer where $S_1 \neq S_2$ measurements of τ_h on opposite sides of the same spot give two different values, $\tau_{h,1}$ and $\tau_{h,2}$. Whereas the measurement of $\tau_{h,1}$ and $\tau_{h,2}$ gives certain information about the wafer and its surfaces, it is not sufficient to determine the three independent parameters S_1 , S_2 and τ_b .

In order to determine S_1 , S_2 and, phase measurements at three different frequencies would be sufficient if the measurement would be sufficiently accurate. At the present state of the art the maximum error in a phase measurement is estimated to be 0.6° . In order to increase the amount of information from the wafer the phase-shift is measured as a function of the frequency. For a spot on the wafer this measurement of $\phi(\omega)$ is performed from opposite sides, so two curves $\phi(\omega)$ are obtained.

Fig. 4 shows the measurement of the two $\phi(\omega)$ curves. The intensity of the light of the lasers is indicated on the graphs. In measurement A the light from the top laser is modulated and the intensity from the bottom laser is held constant. In measurement B the situation is reversed.

Fig. 5 shows the calculated $\phi(\omega)$ relations for four different sets of parameters S_1 , S_2 and τ_b , the thickness of the wafer was $525 \mu\text{m}$ and the diffusion length was $404 \mu\text{m}$ ($\tau_b = 50 \mu\text{s}$) respectively $181 \mu\text{m}$ ($\tau_b = 10 \mu\text{s}$). The influences of surface passivation and variations of τ_b are evident: small phase-shifts correspond to high surface recombination and/or low bulk lifetimes.

By means of analytical expressions for the function $\phi(\omega)$ [8] it can be shown that, given the experimental error, there are sets of (S_1, S_2, τ_b) which give almost the same phase-shift, i.e., the same within the experimental error. For example, the set $(S_1, S_2, \tau_b) = (1000, 2000, 1000)$ and $(663, 1540, 100)$ yield $\phi(\omega)$ curves which differ less than 1.5° . The accuracy can be improved when one of the parameters (S_1, S_2, τ_b) is known and can remain constant in the fit. So when recombination velocities of BSF layers or passivating layers are to be measured on a processed wafer, the lapped side of the wafer is grinded with aluminum oxide powder. This means the bottom side of the wafer is damaged to such an extent as

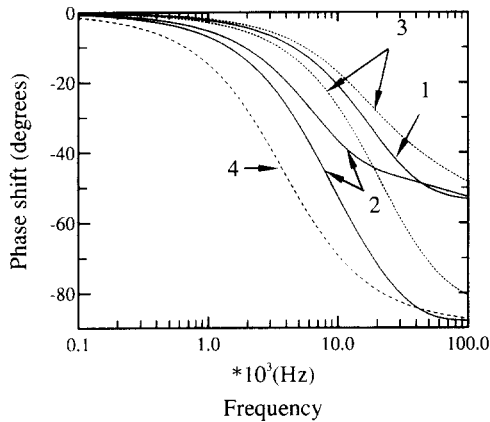


Fig. 5. Phase versus frequency curves for different sets of (S_1, S_2, τ_b) : (1) $(10^7, 10^7, 50)$, (2) $(100, 10^7, 50)$, (3) $(100, 10^7, 10)$, and (4) $(100, 100, 50)$.

to get the maximal surface recombination velocity of $S = 10^7$ cm/s. The recombination velocity on the opposite side and the bulk lifetime are unknown. It is found that good fits can be made with two $\phi(\omega)$ curves and two unknown parameters.

4. Instrumentation

The microwave reflection instrument is drawn schematically in Fig. 2. On top of the antenna lies the silicon wafer, which is illuminated by an infrared light source. The source of light is either an array of 36 infrared Light Emitting Diodes, LEDs, or a diode laser. Through a hole in the antennae the wafer can be illuminated by a second laser from the bottom side, see Fig. 4.

The LEDs, which emit light of wavelength 880 nm, are focused on a spot of approximately 1 cm^2 , with a maximum DC power of 80 mW. For light pulses of short duration and low duty cycle the intensity can be one order of magnitude higher. The transition time of the LEDs is about 600 ns, which means that the minimum decay time which can be measured is about $1 \mu\text{s}$. The light intensity can be modulated harmonically or be pulsed by means of a function generator and a power supply.

The diode laser emits light of 848 nm into a fibre. By means of a focusing lens the spotsize on the wafer can be varied between 0.5 mm and 10 mm. The radiation profile of the antenna is not known, but measurements can be performed with a spotsize of 1 mm. The maximum output power of the diode laser is 200 mW. The laser power supply has a bandwidth of 500 kHz, the transition time is $2.5 \mu\text{s}$. For pulsed light the LEDs are faster.

The microwaves are generated by a 23 dBm (200 mW) phase locked generator at a constant frequency of 2.8 GHz. The power of this signal can be attenuated up to 30 dB. The phase-shift and the attenuation of the signal, which should

compensate the DC part coming from the antenna can be adjusted by a vector modulator, which is controlled by a personal computer. The vector modulator splits the in-going microwave vector in two perpendicular vectors I and Q . Both vectors can be attenuated between 0 and 60 dB by a 12-bit DA converter. The quadrants are selected by a combination of biphasic switches, which are controlled by two additional digital input ports. This means that the out-going microwave signal can be swept over 360° with an resolution better than 0.4° and attenuated up to 60 dB. The insertion loss is 10 dB.

The signal coming out of the vector modulator is added to the signal from the antenna. In order to eliminate the DC signal from the antenna the signal from the vector modulator should have equal amplitude and opposite phase. The correct setting requires fine tuning of the amplitude and phase. Small movements of the wafer on top of the antenna necessitate new adjustment. The correct setting of the digital bits by which the vector modulator is controlled by the personal computer is performed automatically. When the DC part is almost eliminated, the signal is amplified (40 dB) and directed to the detector, which will convert the microwave power signal into a voltage signal.

For decay measurements the voltage signal is registered on a 10 bit 150 MHz LeCroy 9430 oscilloscope, which can also reduce the noise on the signal by averaging a large number of decays.

For the harmonic modulation technique the phase-shift between the detector signal and the light intensity modulation is measured. The phase-shift is a function of the frequency and is to be measured by a EG&G lock-in amplifier model 5302. This instrument has excellent properties for this purpose, such as very good noise suppression and accuracy. The signal from a monitor photodiode inside the housing of the laser diode serves as a reference signal for the lock-in amplifier.

5. Experiments

5.1. Introduction

The microwave reflection instrument is a valuable tool in many different kinds of characterization experiments. In quality control of the production process of solar cells and in basic research experiments it is of key importance to be able to make an estimate of the bulk lifetime τ_b and the surface recombination velocities S_1 and S_2 .

The bulk lifetime depends on the basic material properties, but it can be influenced by gettering and hydrogen passivation. In the case of hydrogen passivation one wishes evidently to separate bulk improvement from surface passivation with hydrogen. Surface recombination can be influenced by several techniques. The main cause of recombination velocity at a silicon wafer surface are unsaturated bonds of silicon atoms. When these bonds are saturated by other atoms, such as oxygen or hydrogen, the recombination rate can decrease very drastically. Thermal oxidation of silicon is known to decrease the recombination velocity. The

Si-oxide, but also Si-nitride, saturates the free bonds at the surface. A HF solution is also known to passivate the surface of silicon wafers, but HF requires special care in an ordinary laboratory. Recently published results on surface passivation by iodine in an ethanol solution showed that this can passivate the surface as well as the HF solution [9].

The measurements of the decay time τ_1 , τ_h or $\phi(\omega)$ curves give information about the quality of the wafer, as the results depend on τ_h , S_1 and S_2 . The recombination rates may lie somewhere in the range between 0 and 10^7 cm/s. This maximum value is determined by the thermal velocity of the carriers. A wafer covered by a native oxide has a recombination rate of typically 10^5 – 10^6 cm/s. In practice it is often seen that the simple model for the recombination proposed in Section 3.3 cannot take account of the real process. For silicon wafers it is often found that the observed value of τ_1 is dependent on the background illumination. This means that the effectiveness of recombination centres and traps in the bulk and on the surface is affected by the concentration of the minorities, i.e., the parameters, S_1 and S_2 in Eqs. (6), (8) and (9) are not constant but depend on $n(x,t)$. For solar cell research it is, therefore, essential to be able to perform measurements with a background illumination up to the intensity of 1 sun.

5.2. Pulsed light

Fig. 6 shows a graph of the microwave signal together with the pulsed light intensity. When the light intensity increases abruptly it will take some time for a steady state carrier concentration to be build up. As the microwave signal is proportional to the instantaneous mean free carrier concentration this response is seen in the reflected microwave signal.

When the light decreases the reflected microwave power decreases almost exponentially to the new steady state level. The decay time after the initial decay is equal to τ_1 . The decay signal is registered by the oscilloscope and is subsequently transmitted to a personal computer, where the general expression

$$f(t) = ae^{-bt} + c \quad (31)$$

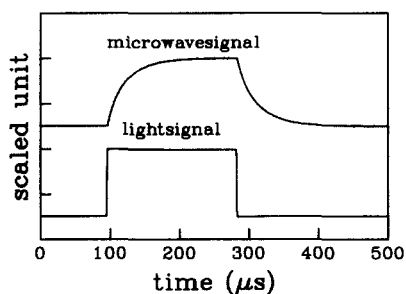


Fig. 6. Light intensity signal and simultaneously recorded microwave signal.

is fitted to the data. The measurement data and the fit results are stored on disk in the PC.

It is possible to make an estimate of the recombination rate of a surface when can be assumed that the recombination velocities on both surfaces of the wafer are practically equal. As an example, a typical experiment using pulsed light will be discussed where the surface was treated with a passivating solution.

A monocrystalline wafer of 525 μm as supplied by the manufacturer shows a τ_1 of 8.7 μs . An oxide layer is grown on the surface by putting the wafer 12 h in a HNO_3 solution. Then the wafer is put inside a teflon container and immersed in a 5% HF solution. The teflon container is put on top of the microwave antenna. The measured increases within a few minutes up to 600 μs . This enormous increase shows that the decay process was initially dominated by the surface recombination rates. The minimum value of τ_b can be put at 600 μs and the maximum value of S in the HF bath is found to be 44 cm/s . The intensity of the incident light should always be such that the measurement is performed under low level injection conditions.

5.3. Harmonic modulation technique

As an example of the harmonic modulation technique an experiment will be described, where the aim is to determine the quality of the surface passivation of an oxide layer on a silicon wafer.

Surface passivation can be achieved by depositing passivating layers in a low-temperature process on the wafer surface [10], [11]. The sample is a p-type monocrystalline $\langle 100 \rangle$ silicon wafer of thickness 525 μm and resistivity 2–5 $\Omega\text{ cm}$. A silicon oxide layer was deposited by a Plasma Enhanced Chemical Vapour Deposition technique using TEOS as a process gas. The oxide layer had a thickness of 135 nm. The lapped side of the wafer was gritted.

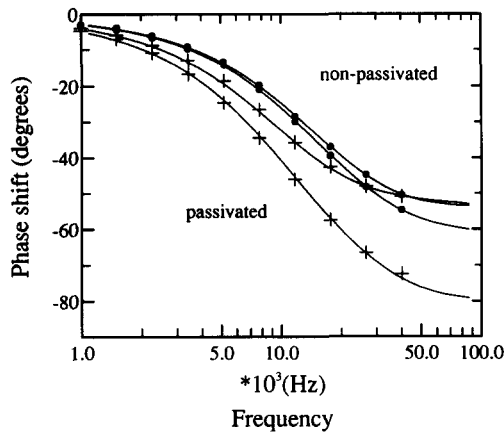


Fig. 7. Effect of silicon oxide passivation.

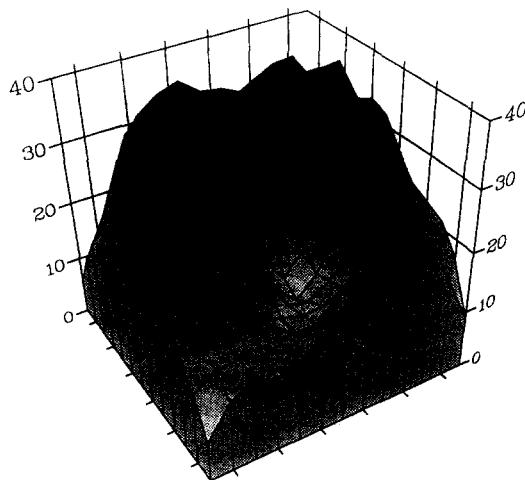


Fig. 8. Mapping of (in μs) of a silicon wafer with a thermal oxide, dimensions $5.4 \times 5.4 \text{ cm}^2$.

The phase versus frequency curves are shown in Fig. 7. After the deposition the recombination velocity of the oxide layer interface was measured to be $S_1 = 1.7(0.2) \times 10^4 \text{ cm/s}$ and the bulk lifetime to be $\tau_b = 135 (27) \mu\text{s}$. The layer had hardly any passivating effect at all. Subsequently the wafer was annealed for 30 min in a forming gas (10% H_2 , 90% N_2). The measurement was performed thirty minutes after the anneal. It was found that $S_1 = 1530 (80) \text{ cm/s}$ and $\tau_b = 150 (30) \mu\text{s}$. Clearly the Forming Gas Anneal (FGA) had improved the surface passivation. This passivating effect proved to be ephemeral however. Fig. 7 too shows the phase curves (upper) that were measured one day after the FGA. The surface recombination velocity had increased to $S_1 = 1.1(0.1) \times 10^4 \text{ cm/s}$. The bulk lifetime was measured to be $\tau_b = 143 (14) \mu\text{s}$.

Mappings of the wafer properties can be made by mounting the wafer on an XY-table. For every spot on the wafer the two phase versus frequency curves can be measured. As a fast alternative a mapping of τ_h can be made in order to determine the homogeneity of the wafer properties. Fig. 8 shows a mapping of the value of τ_h for a p-type monocrystalline $\langle 100 \rangle$ silicon wafer of thickness $375 \mu\text{m}$. The dimensions are $5.4 \times 5.4 \text{ cm}^2$. It was covered on both sides with a thermal oxide. It shows large lateral variations of the effective harmonic lifetime. Measurements of $\phi(\omega)$ curves can determine whether this is due to variations of the bulk properties or variations of the quality of the thermal oxide.

6. Conclusions

The microwave reflection instrument has great potential for the characterization of semiconductor material. Using pulsed light the decay time of the funda-

mental mode can be measured. Under certain conditions estimates can be made of the bulk mean lifetime and the surface recombination velocity.

The harmonic modulation technique is shown to be more powerful, especially due to the accuracy of the lock-in technique. Measurement and analysis of the phase-shift of the microwave signal with respect to the light signal can determine unknown recombination velocities and bulk lifetimes.

References

- [1] T. Otaredian, S. Middelhoek and M.J.J. Theunissen. The theory and application of contactless microwave lifetime measurement. *Material Sci. Eng. B5* (1990) 151.
- [2] T. Otaredian. Separate contactless measurement of the bulk lifetime and the surface recombination velocity by the harmonic optical generation of the excess carriers. *Solid State Electronics* 36 (1993) 153.
- [3] T. Otaredian. Analysis of microwave scattering from semiconductor wafers. *Solid State Electronics* 36 (1993) 163.
- [4] A. Buczkowski, Z.J. Radzimski, G.A. Rozgonyi and F. Shimura. Separation of the bulk and surface components of recombination lifetime obtained with a single laser/microwave photoconductance technique. *J. Appl. Phys.* 72 (1992) 2873.
- [5] A. Sanders and M. Kunst. Characterization of silicon wafers by transient microwave photoconductivity measurements. *Solid State Electronics* 34 (1991) 1007.
- [6] Keung L. Luke and Li-Jen Cheng. A chemical/microwave technique for the measurement of bulk minority carrier lifetime in silicon wafers. *J. Electrochem. Soc.* 135 (1988) 957.
- [7] U. Creutzburg. *Berührungslose Messverfahren zur bestimmung von Silizium Materialeigenschaften für Solarzellenanwendungen*. Thesis, University of Bremen, Germany, 1991. ISBN 3-18-149021-0, VDI Verlag, Reihe 21, Nr. 90.
- [8] M. Orgeret and J. Boucher. Caractérisation d'un substrat semiconducteur par technique micro-onde et injection photonique. *Revue de Physique Appliquée* 13 (1978) 29.
- [9] T.S. Horányi, T. Pavelka and P. Tüttö. In situ bulk lifetime measurement on silicon with a chemically passivated surface. *Appl. Surface Sci.* 63 (1993) 306.
- [10] C. Leguijt, F.J. Bisschop, P. Lölgen, A.R. Burgers, J.A. Eikelboom, R.A. Steeman, H.S. Wielenga W.C. Sinke, P.M. Sarro, P.F.A. Alkemade and E. Algra. Back-surface and volume recombination in thin solar cells. *Proc. 11th European Photovoltaic Solar Energy Conf., Montreux, 1992*, pp. 458.
- [11] C. Leguijt, P. Lölgen, A.R. Burgers, J.A. Eikelboom, A.S.H. van der Heide, R.A. Steeman, W.C. Sinke, P.M. Sarro, L.A. Verhoef, P-P. Michiels and A. Rohatgi. Stable surface passivation of silicon by low-temperature processing. Paper presented at the 12th European Photovoltaic Solar Energy Conference and Exhibition, April 1994, Amsterdam.